# Episodic Magma Hammers in the Recent Cataclysmic Eruption of Hunga Tonga-Hunga Ha'apai

**Yingcai Zheng** ( yzheng12@uh.edu )
University of Houston https://orcid.org/0000-0001-9179-8940
**Hao Hu**
University of Houston
**Frank Spera**
University of California, Santa Barbara https://orcid.org/0000-0002-6876-9313
**Melissa Scruggs**
University of California, Santa Barbara
**Glenn Thompson**
University of South Florida
**Yuesu jin**
University of Houston
**Thomas Lapen**
University of Houston
**Stephen McNutt**
University of South Florida
**Kyle Mandli**
Columbia University
**Zhigang Peng**
Georgia Tech
**Dave Yuen**
Columbia University

---

**Article**

**Keywords:**

**Posted Date:** June 1st, 2022

**DOI:** https://doi.org/10.21203/rs.3.rs-1639007/v1

# Episodic magma hammers for the recent cataclysmic eruption of Hunga Tonga-Hunga Ha`apai

Yingcai Zheng[1*] and Hao Hu[1], Frank J. Spera[2] and Melissa Scruggs[2], Glenn Thompson[3], Yuesu Jin[1], Tom Lapen[1], Stephen R. McNutt[3], Kyle Mandli[4], Zhigang Peng[5], Dave A. Yuen[4]

[1] Department of Earth and Atmospheric Sciences, University of Houston

[2] Department of Earth Science, University of California, Santa Barbara

[3] School of Geosciences, University of South Florida

[4] Dept of Applied Physics and Applied Mathematics, Columbia University

[5] School of Earth and Atmospheric Sciences, Georgia Institute of Technology

*Corresponding Author: Yingcai Zheng, Department of Earth and Atmospheric Sciences, University of Houston, 3507 Cullen Blvd, Rm.312, Houston, TX, 77204-5007; yzheng12@uh.edu

**The Hunga Tonga-Hunga Ha'apai volcanic eruption is arguably the most explosive since Krakatoa erupted in 1883. Understanding how magma dynamics are regulated by volcanic plumbing systems on timescales of seconds to minutes remains challenging.  Here we identify four similar seismic subevents within a 5-minute interval during the intensifying early eruptive phase. Each subevent is similar in waveform and duration and is characterized by a sequence of four stages, A-D. Initial stage A is marked by an unusual negative P-wave polarity which is best explained by an upward, single-force mechanism at the volcano created by a magma hammer related to a transiently closed or blocked conduit. Renewed high mass flow in the second stage (B) produced a single force down at the volcano which was followed by reverberations that represent stages C and D and recovery to the initial state. This episodic magma hammer model, which is consistent with thermodynamic properties of the multiphase magmatic mixture, yields an estimate of magma mass flow in the conduit that is remarkably consistent with discharge into the atmosphere estimated from satellite imagery of plume heights.**

Hunga Tonga-Hunga Ha'apai (HTHH) volcano erupted paroxysmally on 15 January 2022 generating a spectacular ensemble of planetary-scale signals[1], including: audible sounds heard in New Zealand and Alaska, the tallest recorded volcanic plume (peak height ~ 58 km), >400,000 lighting events, a locally destructive tsunami wave, a global meteotsunami traveling at the speed of sound[2], and infrasound and seismic waves that circled the Earth multiple times[3]. In this study, we address the unusual observations of repeating episodic seismic signals during the early stages of the eruption.

### *Geological Background*

HTHH is one of many island-arc volcanoes formed as a result of fast (200-250 mm/year) subduction of the Pacific Plate beneath the Indo-Australian plate along the Tonga-Kermadec arc[4]. For HTHH magmas, juvenile $H_2O$ concentrations are ~4-5 wt%, reaching saturation at 5-7 km depths[5] (see also Supplementary Information Section 2). Crystallization and the concomitant increase in volatile concentrations lead to the development of magma overpressure and the consequent propagation of magma-filled fractures to the surface[5-8].

### *Timings of various volcanic phenomena*

Historically, HTHH is a large submarine edifice that has experienced small-scale submarine and Surtseyan activity[9-14] between large, caldera-forming eruptions[5] (see Fig.1). The period of activity culminating in the cataclysmic 15 January 2022 eruption began at 1520 UTC on 13 January—producing a 20 cm tsunami and a 20 km tall plume, accompanied by ~190,000 lightning strikes[15]. A short-lived land mass between the islands of Hunga Tonga and Hunga Ha'apai formed during the 2014-15 eruption[9] was partially destroyed by 14 January 2022 activity and totally removed by the 15 January eruption.

The 15 January volcanic eruption did not onset abruptly. Instead, an ensemble of time-transgressive phenomena overlapped (**Fig. 1c**). The USGS reported a M5.8 seismic event with an origin time of 04:14:45 15 January 2022 (UTC), located at 20.546°S, 175.390°E with 0 km depth. This time is not the start time of the eruption, as satellite imagery captured at 0410 UTC shows a rapidly growing volcanic plume already 18 km high—peaking at mesospheric heights of ~58 km at 0430 UTC[1]. Extrapolating the infrasound signals in time and distance back to the volcanic location gives a start time around 0402$\pm$1 UTC[1], which is more consistent with observed plume heights. Both before and after the M5.8 seismic event, residents of nearby Mango Island reported ashfall persisting throughout the night, suggesting an eruption duration of ~12 hrs. Although the precise timing of the symphony of phenomena remains uncertain, an uptick in lightning intensity around 0412 UTC is consistent with a stronger eruptive pulse starting at 0407-0409 UTC (Fig. 1c), allowing for an estimated five-minute delay between plume ascent and lightning onset, consistent with previous studies of volcanic lightning[16,17]. The rapid increase in lightning after 0412 UTC is consistent with high mass flow at the vent around 0408 UTC. These phenomena indicate that the eruption was well underway before the 0415 UTC seismic event analyzed in detail below.

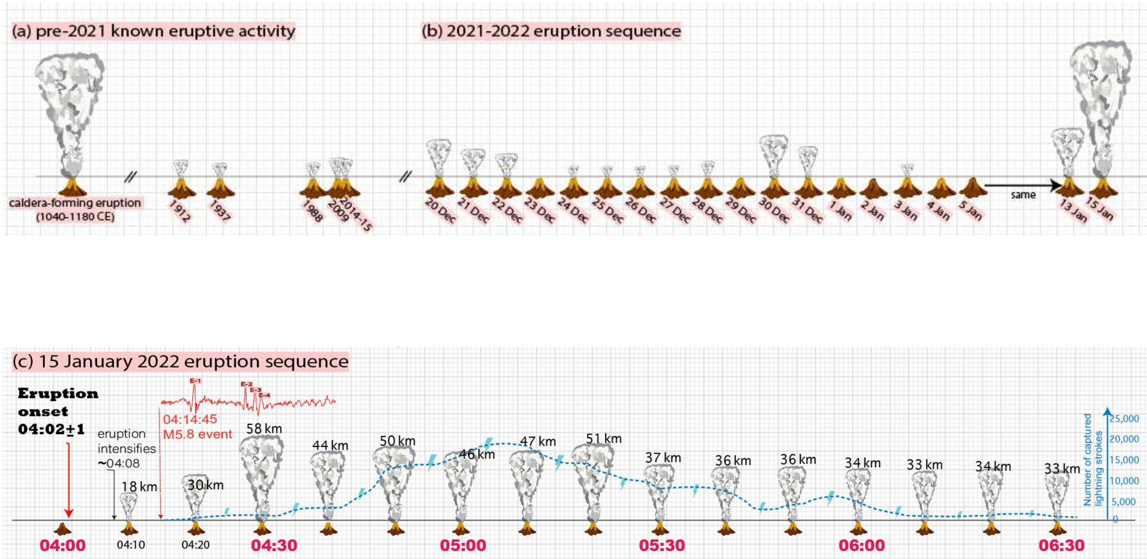


**Figure 1. Timeline of events leading up and including the onset of the 15 January 2022 eruption of HTHH.** Eruption column heights (labeled by numbers) and eruptive history are reported by the Global Volcanism Program[10-15]. For days where no eruptive activity was noted, volcano symbols show no eruption. Days with eruptive activity but no substantial eruption column are marked by lava on the volcano symbols, and eruption columns are to-scale for those days where substantial plume development was reported. Volcanic lightning data are also shown in cyan color[1].

Although a precise collective timeline remains to be refined, the time of the seismic event studied here is in the crescendoing phase of eruptive activity, correlating with peak vent magma discharge. Based on a mean plume-top upward growth rate of 60 m/s, we estimate the time of peak discharge as ~16 minutes before 0430 UTC (or ~0414 UTC), around the time the seismic event occurred.

***Unusual repeating episodic seismic signals***

Our seismic analysis involves limited processing of the raw records. We first downloaded teleseismic waveforms recorded at 417 stations worldwide from Incorporated Research Institutions for Seismology (IRIS), removed their instrumental responses, and lowpass filtered below a corner frequency 0.01 Hz. We computed theoretical travel times of the direct *P* waves for all the stations using the USGS reported origin time and location[18]. Shifted waveforms were stacked and averaged to obtain the seismic wavelet used to study the source process (**Fig. 2; Supplementary Information Fig. S1**).

Within a time of ~300 seconds immediately after the reported seismic event, four subevents—E-1, E-2, E-3, and E-4—are visible in the stacked ground displacement seismogram (**Fig. 2a**). Each subevent has a similar duration of ~25 s. If these were regular earthquakes, a 25 s source duration would result in an event of around Mw7.5, far greater than the reported magnitude M5.8 by USGS. The time intervals between the successive subevents are ~204.6 s (E-1&2), ~39.8 s (E-2&3), and ~25.4 s (E-3&4), respectively. We call the subevents E-1 to E-4 'episodic' because their corresponding waveforms are remarkably similar (**Fig. 2c-e**), indicating that similar eruption dynamics likely governed these subevents.

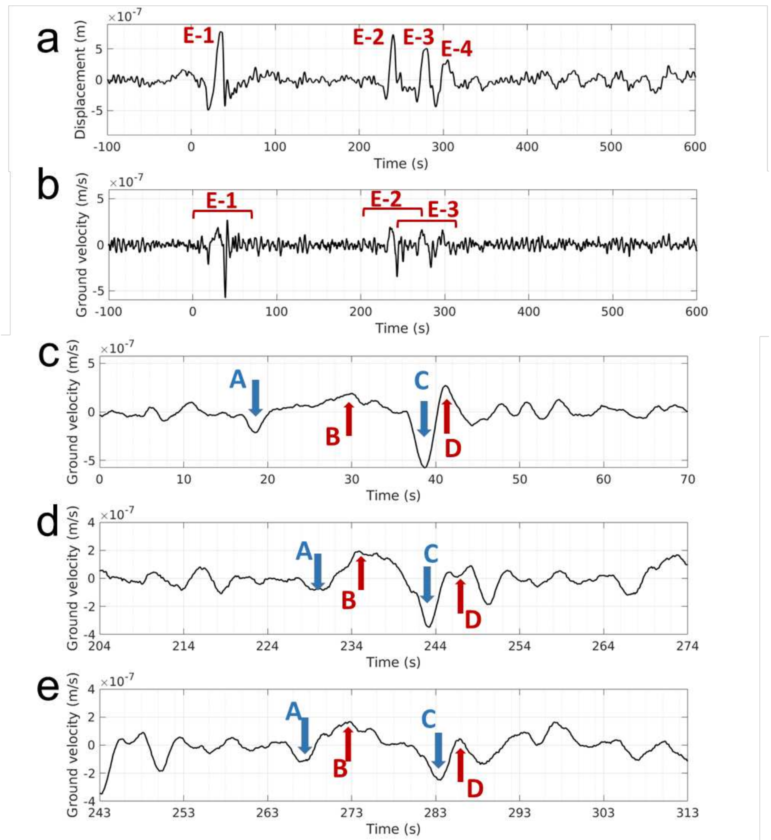


**Figure 2. Source wavelet by stacking global seismic signals.** The vertical-component seismograms are lowpass filtered below a corner frequency 0.01 Hz; (a) stacked ground displacement showing four sub-eruptions, E-1 to E-4; (b) stacked ground velocity seismogram; (c) E-1 velocity waveform; (d) E-2 velocity waveform; (e) E-3 and E-4 velocity waveforms. Color arrows and numbers in (c)-(e) refer to the eruption stages A-D. Time zero corresponds to the USGS reported seismic event origin time 04:14:45 Jan 15 2022.

A puzzling observation is that the polarities of the observed *P*-wave first motions are found to be downward in both the stacked waveform (**Fig. 2**) and the waveforms recorded by all global stations at a wide range of azimuths (**Supplementary Information Fig. S1**). Furthermore, similar waveform stacking procedures for global *S* waves using the S wave theoretical travel times yields no visible energy in the transverse component (see **Supplementary Information Fig. S2**). The stacked P and S wave characteristics suggest that the subevents' seismic signals were not caused by earthquake dislocation faulting, but rather by equivalent forces with azimuthal symmetry. Possible forces consistent with the observed first motion are: (1) a single force in the upward (not downward) direction or (2) an implosion/CLVD[19] source at the volcano. Detailed full-wave seismic modeling showed single forces are preferred over either implosion or CLVD (see **Supplementary Information Sec. 1**). Both the implosion and CLVD source near a free surface produce strong P-to-S converted waves not observed in the seismic records (see **Supplementary Information Fig. S3-8**). Our discussions below are based on a single-force model for the seismic source and the modeled force time history (see **Supplementary Information** Fig. S9).

***Eruption stages and magma hammer mechanism***

Based on the stacked P-wave seismograms (**Fig. 2b-e**), we can decipher four eruptive stages (A, B, C and D) within each of the four subevents. Because each of the seismic subevents exhibits similar waveforms, we focus our analysis on the E-1 time series (**Fig. 3a**) in the context of the magma transport system, particularly the stage dynamics inferred from the seismic record (**Fig. 3b-g**). The durations for Stages A-D are ~3s, 15s, 3s, and 3s, respectively. The timing of E-1A is ~ 4:15:00, 15 seconds after the reported seismic events[20].

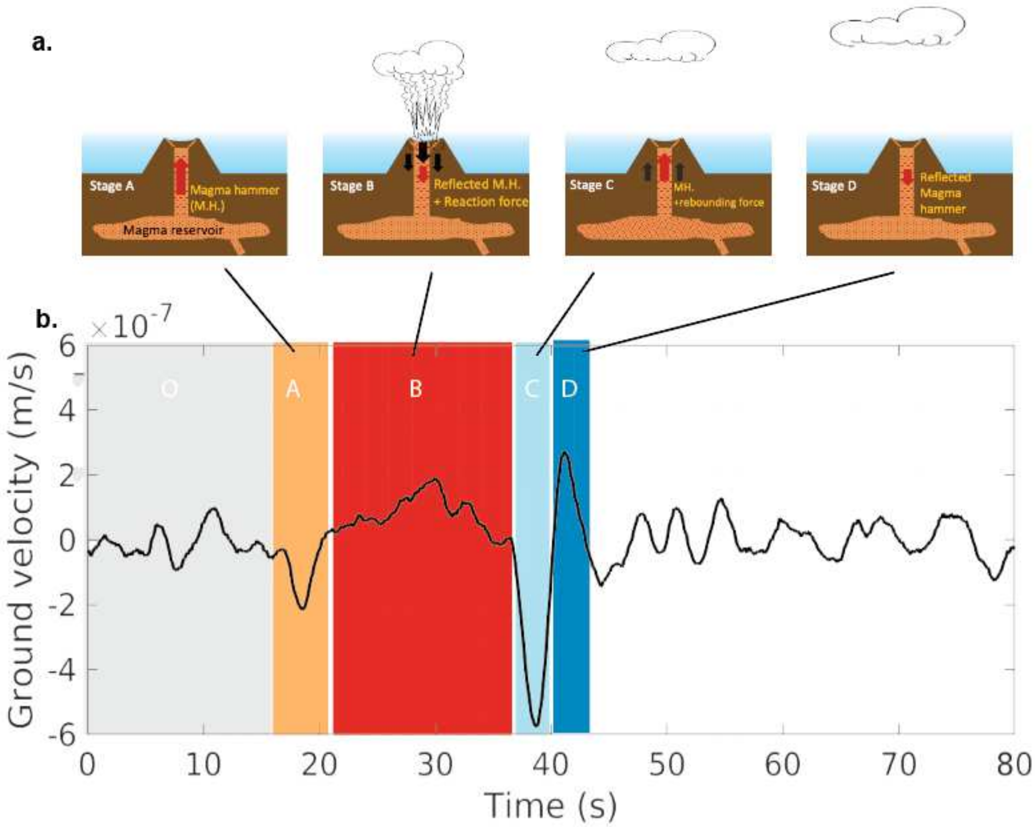


**Figure 3. Eruption stages and magma plumbing system.** (a) Volcano-reservoir schematics of states and forces (red arrow: magma hammer; black arrow: reaction force) corresponding to Stages A-D. Magma reservoir centered at depth of 5-8 km is based on geobarometry[5]. (b) Globally stacked ground velocity (vertical component) of event E-1. Time zero corresponds to ~04:14:45 Jan 15, 2022.

Before Stage-A (time <15s in the record), the stacked seismic record is characterized by fluctuating ground motion (**Fig. 3b**) likely associated with magma movement in the conduit, possible phreatomagmatic activity and magma venting. As presented above, infrasound and lightning data indicate that eruption intensity (the mass discharge at the vent) likely accelerated in the interval 0402-0415 UTC, at which time event E-1 occurred.

***Stage A: magma hammer and estimates of magma flux and discharge***

Stage-A (E-1A) lasted about ~3.2 s and was characterized by a distinct downward ground motion at the seismometers, meaning that the seismic source was either an upward single-force or a magma reservoir contraction (implosion source) at the volcano. Full-wave seismic modeling (Supplementary Information Section 1) reveals that an upward single-force source, with a force magnitude ~ $5.0 \times 10^{12} N$ in Stage-A, fits the data far better than an implosion or CLVD source (**Supplementary Information Sec. 1; Fig. S3-S8**). The May 1980 Mount St. Helens (MSH) eruption was also found to produce single forces for seismic wave generation[21]. Unlike the 1980 MSH eruption, ground motion in Stages A and C for all four seismic subevents (E-1~E-4) of the 15 January 2022 HTHH eruption was an upward single force at the volcano. A plausible mechanism to explain this upward force is the water-hammer[22-24].

- Magma hammer and piston motion

In the conventional water-hammer mechanism, water flows steadily through a pipe with an open valve. Rapid closure of this valve creates a surge of water hammer pressure $P_H$, acting on the closure which can sometimes burst a steel pipe. Here, we sketch the basic water-hammer concept, modified to the parameters of a multi-phase magma.

Mathematically, the water-hammer pressure, $P_H$, can be described by the well-known Joukowsky equation [22] for slow fluid flow (V<< c): $P_H = \rho c V$, where $\rho$ is the fluid density, $c$ is the sound speed in the fluid, and $V$ is the fluid flow speed in the pipe. This equation is also used to compute the pressure exerted on a piston of fluid impacting on a flow stoppage surface. Since magma is involved here rather than water, we apply the term ***magma hammer*** to describe this process. Because eruptive activity began ~10 minutes before subevent E-1, a magma transport conduit connected to a surface vent and the plume was likely established. Multiplying both sides of the above equation by the cross-sectional area, $A$, of the flow conduit, $F_H = P_H A = \rho c Q_V = c Q_m$, where the hammer force, $F_H$, can be directly estimated by the seismic modeling (~ $5 \times 10^{12}$ $N$ for Stage-A), $Q_V = VA$ is the magma volume flux (in $m^3/s$), and $Q_m = \rho V A$ is the magma mass flux (in kg/s), in the subsurface plumbing system. It is important to note that in this expression the density is that of the magmatic mixture of melt plus fluid. This quantity varies considerably as does the sonic velocity of the magma because the fluid fraction in the mixture increases rather strongly upon decompression as magma flows up the conduit towards the surface vent (see **Supplements Information Sec. 2 and Sec. 3** for details).

- Equation of state and flux estimate

To apply the water hammer idea to the situation at HTHH, the density and sound wave velocity of the multi-phase magmatic mixture are required. These in turns require consideration of magma composition, degree of volatile saturation, and flow regime. Equilibrium crystallization of last-erupted HTHH andesites was modeled using rhyolite-

MELTS [25] to approximate the state of an andesitic magma as it undergoes closed-system degassing and ascends adiabatically to the surface from a reservoir depth of ~7.5 km (P = 2 kbar). The state of the magma body was recorded at each *P-T along an isentropic path* and the volume fraction of the exsolved volatiles calculated (**Supplementary Information Sec. 2; Fig.S10-11)**. The sonic velocity of a two-phase (melt+fluid) mixture was then computed for both bubbly flow (i.e., well mixed) and slug flow (i.e., gas pockets) regimes (see details in **Supplementary Information Sec. 3, Fig.S12-13**). We argue that slug flow is more likely, given the explosiveness of the eruption and short time scales involved. Taking $c \sim 1500$ m/s, we can get a mass flux $Q_m \sim 3.3 \times 10^9$ kg/s using the peak force in E-1A. Approximating the seismic wavelet in E-1A as a triangle, the average force should be halved. Therefore, the average magma mass flux is about $\bar{Q}_m \sim 1.6 \times 10^9$ kg/s. Alternatively, we can estimate the volcanic discharge into the atmosphere [26]. According to satellite images of the volcanic plume heights, the mass flow to support a 58 km volcanic plume from Yuen et al. [1] is ~ $1.4 \times 10^9$ kg/s. Considering the uncertainties, the mass flow estimated by our magma-hammer model is of the same order of magnitude as those required to attain peak plume heights.

Our proposed magma-hammer model is consistent with the seismic data, discharge estimate, physiochemical magma properties, and sonic velocities. We argue that Stage A of E-1~E-4 with similar ground displacements represents magma hammer breaching of a short-lived blockage of the magma conduit, generating an upward single force.

***Stage B***

Stage E-1B – a downward single force at the volcano—corresponds mainly to the reactive impulsive force associated with reopening of the magmatic conduit and reestablishment of intense outflow for ~15 s (**Fig. 3a)**. The eruption could have sent a series of pulses of volcanic product (ash, pyroclasts, crystals, lithics and seawater-derived steam) into the atmosphere based on observed maximum plume heights referred to earlier. This 'upside-down rocket'-type eruption created a downward single-force on the order of $\sim 9 \times 10^{12}$ N. The magnitude of the force is comparable to that of the MSH eruption [21] of $\sim 10^{13}$ N.

***Stages C and D***

Stage E-1C, initiated about 20 s after the onset of E-1A, exhibits an upward force of $\sim 4 \times 10^{12}$ N, which we associate with a second-phase closing of the conduit and subsequent generation of a magma-hammer upward force (details in **Supplementary Information Sec. 3**). Stage E-1C (**Fig. 3a**) and Stage E-1D (**Fig. 3a**) do not mirror or repeat the Stage-A to Stage-B pattern because E-1D is only ~3s but E-1B is ~15s. Stage E-1B exerted a sustained downward force, probably depressing both the magma in the conduit and the magma chamber and surrounding rock. It is likely that Stage E-1C is a magma-hammer force related to the backflow impacting the overburden rock. E-1D represents a reflected magma-hammer signal traveling down to impact the magma reservoir that created a downward force. Stages E-1C and E-1D represent one cycle of oscillatory piston motion as magma travels through the conduit, from the reservoir to the surface. The ~6s period corresponds to the two-way travel time of the magma-hammer signal in the conduit. Taking an estimated average traveling sonic velocity of ~2,000 m/s, we can determine the depth of the magma chamber at ~6 km, consistent with geobarometric estimates [5].

**Repeating episodic seismic signals**

Stages A-D for the E-1 event were repeated three more times (Fig.2), each of which can be interpreted similarly to the E-1A to E-1D sequence of UP-DOWN-UP-DOWN forces, by virtue of similar waveforms. These large magnitude forces are short in duration and could produce loud audible sounds as recorded by observers and infrasonic sensors around the world[1]. The timings of the seismic energy envelopes of E-1~E-4 and those of the air pressure waveform recorded by Station MSVF in Fiji are in good agreement [1].

***Conclusions***

The HTHH eruption will be an important event in volcanology and other geosciences. It is unusual that a volcanic eruption could generate such energetic P waves with negative polarities worldwide. It is even more astonishing that HTHH has a sequence of four similar episodic events, separated in time by only tens of seconds, in the early intensifying phase of the eruption. It reveals a rapid but regulated nature of the shallow magma transport system manifested as repeating magma hammers due to brief (order seconds) cessation of magma flow in the conduit. Our scenario is consistent with available seismic, infrasound, lightning, and satellite data. It is also consistent with the mechanics and thermodynamics of magma under subsurface conditions accounting for the variation in the volume fraction of fluid—mainly supercritical $H_2O$—in the magma. Examination and modeling of the seismic data suggest that HTHH produced the largest known magma-hammer force associated with a violent volcanic eruption.

The eruptive volume of the epic 15-Jan-2022 HTHH event is presumably a small portion of the total available magma in the reservoir that, in turn, is repeatedly recharged by additions from below. Future work will benefit from new 3D marine seismic imaging of the plumbing system, with the goal of imaging not only the magma reservoir at 5-8 km depth but also the size and geometry of the plexus of magma conduits to further test our model and perhaps constrain the timing, duration, and magnitude of a future catastrophic eruption using the episodic nature of the system.

STOP STOP STOP STOP  STOP STOP STOP STOP

## References

1 Yuen, D. A. *et al.* Under the Surface: Pressure-Induced Planetary-Scale Waves, Volcanic Lightning, and Gaseous Clouds Caused by the Submarine Eruption of Hunga Tonga-Hunga Ha'apai Volcano. *Earthquake Research Advances*, 100134, doi:https://doi.org/10.1016/j.eqrea.2022.100134 (2022).

2 Carvajal, M., Sepúlveda, I., Gubler, A. & Garreaud, R. Worldwide Signature of the 2022 Tonga Volcanic Tsunami. *Geophys. Res. Lett.* **n/a**, e2022GL098153, doi:https://doi.org/10.1029/2022GL098153 (2022).

3 Amores, A. *et al.* Numerical Simulation of Atmospheric Lamb Waves Generated by the 2022 Hunga-Tonga Volcanic Eruption. *Geophys. Res. Lett.* **49**, e2022GL098240, doi:https://doi.org/10.1029/2022GL098240 (2022).

4 Smith, I. E. M. & Price, R. C. Tonga-Kermadec arc and Havre-Lau back-arc system: Their role in the development of tectonic and magmatic models for the western Pacific. *Journal of Volcanology and Geothermal Research* **156**, 315-331 (2006).

5 Brenna, M. *et al.* Post-caldera volcanism reveals shallow priming of an intra-ocean arc andesitic caldera: Hunga volcano, Tonga, SW Pacific. *Lithos* **412-413**, 106614, doi:https://doi.org/10.1016/j.lithos.2022.106614 (2022).

6 Tait, S., Jaupart, C. & Vergniolle, S. PRESSURE, GAS CONTENT AND ERUPTION PERIODICITY OF A SHALLOW, CRYSTALLIZING MAGMA CHAMBER. *Earth Planet. Sci. Lett.* **92**, 107-123 (1989).

7 Lister, J. R. & Kerr, R. C. Fluid-mechanical models of crack propagation and their application to magma transport in dykes. *Journal of Geophysical Research: Solid Earth* **96**, 10049-10077, doi:10.1029/91JB00600 (1991).

8 Fowler, S. J. & Spera, F. J. Phase equilibria trigger for explosive volcanic eruptions. *Geophys. Res. Lett.* **35**, doi:https://doi.org/10.1029/2008GL033665 (2008).

9 Cronin, S. J. *et al.* New volcanic island unveils explosive past, Eos, 98, https://doi.org/10.1029/2017EO076589. Published on 26 June 2017., (2017).

10 Global Volcanism Program. Report on Hunga Tonga-Hunga Ha'apai (Tonga). In McClelland, L., (ed.). *Scientific Event Alert Network Bulletin* **13:5**, Smithsonian Institution, https://doi.org/10.5479/si.GVP.SEAN198805-243040, doi: https://doi.org/10.5479/si.GVP.SEAN198805-243040 (1988).

11 Global Volcanism Program. Report on Hunga Tonga-Hunga Ha'apai (Tonga). In: Venzke, E.A. and Wunderman, R. (eds.), . *Scientific Event Alert Network Bulletin* **34(2)**, Smithsonian Institution, doi: 10.5479/si.GVP.BGVN200902-243040, doi: https://doi.org/10.5479/si.GVP.SEAN198805-243040 (2009).

12 Global Volcanism Program. Report on Hunga Tonga-Hunga Ha'apai (Tonga). In: Venzke, E.A. and Wunderman, R. (eds.). *Scientific Event Alert Network Bulletin* **34(3)**, Smithsonian Institution. https://doi.org/10.5479/si.GVP.BGVN200903-243040, doi: https://doi.org/10.5479/si.GVP.SEAN198805-243040 (2009).

13 Global Volcanism Program. Report on Hunga Tonga-Hunga Ha'apai (Tonga). In Wunderman, R. (ed.). *Scientific Event Alert Network Bulletin* **40(1)**, Smithsonian Institution. doi: 10.5479/si.GVP.BGVN201501-243040., doi: https://doi.org/10.5479/si.GVP.SEAN198805-243040 (2015).

14 Global Volcanism Program. Report on Hunga Tonga-Hunga Ha'apai (Tonga). In: Crafford, A.E., and Venzke, E. (eds.). *Scientific Event Alert Network Bulletin* **47(2)**, Smithsonian Institution, doi: 10.5479/si.GVP.BGVN202202-243040., doi: https://doi.org/10.5479/si.GVP.SEAN198805-243040 (2022).

15 Global Volcanism Program. Report on Hunga Tonga-Hunga Ha'apai (Tonga). In: Sennert, S.K. (ed.). *Weekly Volcanic Activity Report, 12 January – 18 January 2022*, Smithsonian Institution and U.S. Geological Survey, doi: https://doi.org/10.5479/si.GVP.SEAN198805-243040 (2022).

16 Hoblitt, R. P. An Experiment to Detect and Locate Lightning Associated with Eruptions of Redoubt Volcano. *Journal of Volcanology and Geothermal Research* **62**, 499-517 (1994).

17 Behnke, S. A. *et al.* Observations of volcanic lightning during the 2009 eruption of Redoubt Volcano. *Journal of Volcanology and Geothermal Research* **259**, 214-234 (2013).

18 Yu, C., Zheng, Y. & Shang, X. Crazyseismic: A MATLAB GUI-Based Software Package for Passive Seismic Data Preprocessing. *Seismol. Res. Lett.* **88**, 410-415, doi:10.1785/0220160207 (2017).

19 Knopoff, L. & Randall, M. J. Compensated Linear-Vector Dipole - a Possible Mechanism for Deep Earthquakes. *J. Geophys. Res.* **75**, 4957-& (1970).

20 USGS. M5.8 Volcanic Eruption - 68 km NNW of Nuku'alofa, Tonga, https://earthquake.usgs.gov/earthquakes/eventpage/us7000gc8r/executive Accessed 15 Feb 2022. (2022).

21 Kanamori, H. & Given, J. W. ANALYSIS OF LONG-PERIOD SEISMIC-WAVES EXCITED BY THE MAY 18, 1980, ERUPTION OF MOUNT ST HELENS - A TERRESTRIAL MONOPOLE. *J. Geophys. Res.* **87**, 5422-5432, doi:10.1029/JB087iB07p05422 (1982).

22 Streeter, V. L. & Wylie, E. B. Waterhammer and Surge Control. *Annu Rev Fluid Mech* **6**, 57-73, doi:10.1146/annurev.fl.06.010174.000421 (1974).

23 Lawrence, W. S. & Qamar, A. Hydraulic Transients: A Seismic Source in Volcanoes and Glaciers. *Science* **203**, 654-656, doi:10.1126/science.203.4381.654 (1979).

24 Kieffer, S. W. SEISMICITY AT OLD FAITHFUL GEYSER - AN ISOLATED SOURCE OF GEOTHERMAL NOISE AND POSSIBLE ANALOG OF VOLCANIC SEISMICITY. *Journal of Volcanology and Geothermal Research* **22**, 59-95, doi:10.1016/0377-0273(84)90035-0 (1984).

25 Gualda, G. A. R. & Ghiorso, M. S. MELTS_Excel: A Microsoft Excel-based MELTS interface for research and teaching of magma properties and evolution. *Geochemistry, Geophysics, Geosystems* **16**, 315-324, doi:https://doi.org/10.1002/2014GC005545 (2015).

26 Carey, S. & Bursik, M. in *The Encyclopedia of Volcanoes (Second Edition)* (ed Haraldur Sigurdsson) 571-585 (Academic Press, 2015).

## Acknowledgments

Funding sources from U.S. NSF and DOE will be provided later.

## Data availability

Seismic data are downloaded from IRIS. The facilities of IRIS Data Services, and specifically the IRIS Data Management Center, were used for access to waveforms, related metadata, and/or derived products used in this study. IRIS Data Services are funded through the Seismological Facilities for the Advancement of Geoscience (SAGE) Award of the National Science Foundation under Cooperative Support Agreement EAR-1851048.

## Author Contribution Statement

From ~February 1 to May 3, the authors held weekly Zoom meeting discussions. DAY is instrumental in forming the team. This manuscript is a result of this effort. An initial manuscript draft was provided by YZ. All the authors contributed to writing. YZ identified the 4 episodic events. HH did seismic modeling (SI Sec. 1) and Fig. 2. FJS led the effort in the magma hammer modeling in SI Sec. 3 and plume height analysis. MS led geological/petrological evaluation of HTHH, the timeline in Fig. 1, and rhyolite-MELT's modeling of magma mixture (in SI Sec. 2). GT led the infrasound and lightning record analysis for the eruption timeline. TJL and YJ suggested the water hammer idea. SRM contributed to eruption sequence/timeline analysis. KM studied tsunami records and contributed to the eruption timeline. ZGP contributed to the seismic analyses. All authors participated in the weekly discussions which have shaped the manuscript to its current form.

**Competing interests**

The authors declare no competing interests.

# Supplementary Files

This is a list of supplementary files associated with this preprint. Click to download.

- SupplementaryInformation.pdf
- Supplementarydata.xlsx